Double stars with wide separations in the AGK3 – II. The wide binaries and the multiple systems

J.-L. Halbwachs, M. Mayor, S. Udry

Monthly Notices of the ROYAL ASTRONOMICAL SOCIETY
MNRAS **464,** 4966–4976 (2017) doi:10.1093/mnras/stw2683

Double stars with wide separations in the AGK3 – II. The wide binaries and the multiple systems*

J.-L. Halbwachs,[1]★ M. Mayor[2] and S. Udry[2]

[1]*Observatoire astronomique de Strasbourg, Université de Strasbourg, CNRS, UMR 7550, 11 rue de l'Université, F-67000 Strasbourg, France*
[2]*Observatoire Astronomique de l'Université de Genève, 51, chemin des maillettes, CH–1290 Sauverny, Switzerland*

Accepted 2016 October 14. Received 2016 October 13; in original form 2016 August 29

ABSTRACT

A large observation programme was carried out to measure the radial velocities of the components of a selection of common proper motion (CPM) stars to select the physical binaries. 80 wide binaries (WBs) were detected, and 39 optical pairs were identified. By adding CPM stars with separations close enough to be almost certain that they are physical, a bias-controlled sample of 116 WBs was obtained, and used to derive the distribution of separations from 100 to 30 000 au. The distribution obtained does not match the log-constant distribution, but agrees with the log-normal distribution. The spectroscopic binaries detected among the WB components were used to derive statistical information about the multiple systems. The close binaries in WBs seem to be like those detected in other field stars. As for the WBs, they seem to obey the log-normal distribution of periods. The number of quadruple systems agrees with the no correlation hypothesis; this indicates that an environment conducive to the formation of WBs does not favour the formation of subsystems with periods shorter than 10 yr.

Key words: binaries: general – stars: formation – stars: solar-type.

1 INTRODUCTION

Binary stars cover a very wide range of separations, from a few stellar radii to thousands of astronomical units. The binaries with orbital period comparable to a human lifetime are detected from variations of quantities such as the radial velocity or the position of the components, but the wide binaries (WBs) are more hazardous to identify. Both components look like single stars with constant velocities, and statistical criteria are used to infer whether they can be bounded by gravitation.

The origin of WBs is still debated, since they cannot be obtained from the simple fragmentation of a collapsing cloud of gas and dust. Other processes have been proposed, such as gravitational perturbations from passing stars and giant molecular clouds (Weinberg, Shapiro & Wasserman 1987; Jiang & Tremaine 2010), star cluster dissolution (Kouwenhoven et al. 2010) and the dynamical evolution of triple systems (Reipurth & Mikkola 2012). This motivates investigations about the statistical properties of these systems, which are assumed to contain the signature of their formation (see the review by Duchêne & Kraus 2013, and references therein).

The components of WBs are not all single stars, but some of them are binaries with closer separation. The properties of the multiple systems, and the possible correlation between the parameters of the WBs and those of the inner binaries, are also clues to understanding the origin of these objects. In addition to research mentioned in Duchêne & Kraus (2013), these questions were investigated recently by Tokovinin (2014, 2015), and by Riddle et al. (2015). They estimated that the frequency of inner binaries is the same among the primary and among the secondary components of the WBs, but that the frequency of quadruple systems is too large to assume that the presence of inner binaries is not correlated. If this is confirmed, the formation of the inner binaries could result from the environment where the WB was formed.

In this paper, we provide a new sample of WBs to derive their statistical properties. Since the number of optical stars grows as the square of the apparent separations, the selection of physical WBs is based on more parameters. One of us (Halbwachs 1986, hereafter H86) used the proper motion to select 439 common proper motion (CPM) pairs from the reduction of the second and of the third Astronomischen Gesellschaft Katalog (AGK2/3) by Lacroute & Valbousquet (1974). These wide pairs were listed in two tables, according to the time $T = \theta/\mu$, where θ is the apparent separation and μ the proper motion. Therefore, T is the time it takes for the proper motion to displace the components over a distance equal to their separation. The first table contains 326 pairs of stars with $T < 1000$ yr, and the second one contains 113 pairs with T between 1000 and 3500 yr. To avoid any confusion between the tables in H86 and those in the present article, tables I and II of H86 are called, respectively, list 1 and list 2 hereafter. The rate of optical pairs was estimated to be around 1 per cent in list 1, and 40 per cent in list 2.

An observational programme was initiated in 1986 to measure the radial velocities (RVs) of the stars, and to select the physical binaries. However, several WBs are in fact multiple systems

* Based on observations performed at the Observatoire de Haute–Provence (CNRS), France

★ E-mail: jean-louis.halbwachs@astro.unistra.fr

Table 1. Sample of the RV catalogue. It shows the headers of the first stars, beginning with the number of the list in H86, the sequential number of the pair, and a capital letter designating the component. In the catalogue file, each header is immediately followed by N_{meas} measurements. The full catalogue is available as supporting information with the electronic version of the article.

CPM	AG	HIP/HD/BD/AG	$B-V$ (mag)	N_{meas}	$\bar{V}$ (km s^{-1})	$\sigma_{\bar{V}}$ (km s^{-1})	$P(\chi^2)$	J2000 coordinates (HH mm s.sss)	(±DD mm s.ss)
2 1A	+17 8	HIP 493	0.60	7	−45.277	0.139	0.679	00 05 54.748	+18 14 06.02
2 1B	+17 9	HIP 495	0.92	4	−44.973	0.189	0.956	00 05 55.473	+18 04 33.14
2 3A	+24 37	BD+23 45	1.40	4	−53.179	0.161	0.744	00 22 42.473	+24 34 08.34
2 3B	+24 36	BD+23 44	0.58	4	−20.225	0.244	0.670	00 22 37.298	+24 33 45.75

including close binaries (CBs), and the RVs of 66 stars from the two lists appeared to be variable, or possibly variable. These 66 stars were observed over about 20 yr, leading to the derivation of the orbital elements of 52 short-period spectroscopic binaries (SBs), and the confirmation of periods of a few decades for 11 other stars. The status of the three remaining stars is uncertain, and the variability of their RV is questionable. These results were published in Halbwachs, Mayor & Udry (2012, hereafter Paper I).

The present paper is the continuation of Paper I. It is organized as follows. The observation programme and the mean RVs of the component stars are presented in Section 2. The selection of the physical binaries is in Section 3. A bias-controlled sample of WBs with unevolved components is presented in Section 4. This sample is used to derive the frequency of WBs in Section 5. Some properties of the multiple systems are investigated in Section 6. Section 7 is the conclusion.

2 THE RADIAL VELOCITY MEASUREMENTS

The observational programme was detailed in Paper I. In summary, we used the spectrovelocimeter CORAVEL (for Correlation Radial Velocities, Baranne, Mayor & Poncet 1979), which was installed on the Swiss 1-m telescope at the Observatory of Haute-Provence until its decommissioning in 2000. Our list of targets contained 266 stars from the two lists of H86. Since the probability of being physical is much larger for a pair in list 1 than in list 2, only 90 targets were chosen among the 326 pairs of list 1: the systems with T shorter than 350 yr were discarded, since the expected number of optical systems among them is only 0.5, leading to a frequency of 0.2 per cent. We discard also the pairs with both components fainter than the completeness limit of AGK2/3, which is $m_{pg} = 9.1$ mag. Moreover, the 113 pairs in list 2 provided 176 targets. Due to the limitations of CORAVEL, these stars are generally as late as or later than F5, but a few Am-type stars were also observed. The precision of CORAVEL was around 0.3 km s^{-1} for slow rotators with spectral types around K0, but around 1 km s^{-1} for Am stars.

The detection of the SBs was based on the $P(\chi^2)$ test at the 1 per cent threshold. The measurements of the 66 stars suspected to be variable were presented in Paper I. The 200 remaining had a total of 1473 RV measurements, but the number of measurements is not the same for every star: three early-type stars were observed only once, and another one had only two measurements. In contrast, the RV of 52 stars was obtained at least 10 times, usually because the other component of the pair had a variable RV. Among the 200 stars not discussed in Paper I, 98 were observed at least five times. The median time-span of the observations is 1720 d.

The RV catalogue is in electronic form, in one plain text file. The format is the same as for the RV catalogue in Paper I. For each star, the RV measurements are preceded by a header, providing the number of RV measurements and the mean RV. The format of the headers is presented in Table 1, and that of the measurements is in Table 2.

Table 2. Sample of the RV catalogue. The measurements of star 2:1A, following the header.

JD +2 400 000	V_R (km s^{-1})	σ_{RV} (km s^{-1})	T
46 429.272	−45.28	0.41	C
46 729.412	−45.05	0.39	C
46 770.322	−44.99	0.38	C
46 814.230	−45.07	0.37	C
47 364.626	−45.06	0.39	C
48 138.550	−45.54	0.37	C
48 881.719	−45.70	0.31	C

Taking into account the SBs in Paper I, the mean RVs are available for both components of 119 CPM systems. The selection of the physical pairs is discussed in the next section.

3 SELECTION OF THE WIDE BINARIES OBSERVED WITH CORAVEL

We consider now the 119 CPM systems observed with CORAVEL. The selection of the binary stars is essentially based on the difference between the RVs of the components. In addition, the trigonometric parallax of 131 stars was measured thanks to the *Hipparcos* satellite (for High Precision Parallax Collection Satellite; ESA 1997; van Leeuwen 2007), including both components of 44 pairs. Therefore, the binaries are selected based on the RVs for the 119 pairs, but also based on the parallaxes for 44 of them. This last criterion leads to the detection of only two optical pairs with compatible RVs: 2:87 and 2:99.

The compatibility of the RVs is verified as follows. When both components have the same RV in reality, 99 per cent of the pairs are expected to satisfy the condition $\|\Delta V\| < 2.575\sigma_{\Delta V}$, where ΔV is the RV difference and $\sigma_{\Delta V}$ its uncertainty. However, two additional tolerances are added:

(i) We take into account the contribution of the orbital motion. This term cannot be derived exactly, since we do not know the orbital parameters, but it is always less than the escape velocity corresponding to a parabolic motion. We add then:

$$V_{escape} = 42.23 \times \sqrt{\frac{\mathcal{M}_A + \mathcal{M}_B}{s}} \quad (1)$$

where $\mathcal{M}_A$ and $\mathcal{M}_B$ are the masses of the components, in solar units, and s the projection of the separation between the components, in astronomical units. The derivation of $\mathcal{M}_A$, $\mathcal{M}_B$ and s is explained later in the present section. The coefficient 42.23 is used to derive V_{escape} in km s^{-1}. For s larger than 1000 au, V_{escape} is less than about 2 km s^{-1}.

(ii) We add an allowance to take into account the difference between the spectral types of the components. Thanks to the correction of the RVs related to the $(B-V)$ colour indices, this error is rather small, and an additional tolerance of 0.11 km s^{-1} is assumed. This term leads to the selection of five additional binaries.

In addition to the apparent separation between the components, three parameters are needed to derive $V_{\rm escape}$ according to equation (1): the masses of the components, and the distance of the system. To derive them, the spectral types and the B and V magnitudes are obtained from the Simbad data base (Wenger et al. 2000).[1] When B is missing in Simbad, it is derived from the Tycho B_T and V_T magnitudes (ESA 1997). The mass of each component is derived from the spectral type, but the luminosity class is often missing. When the trigonometric parallax is known, the luminosity class is derived from the absolute magnitude. Otherwise, we assume that both components are dwarfs when the spectral type of the brightest one is earlier than that of the other, or when the $(B-V)$ colour index of the brightest one is the smallest. We do not take into account the luminosity class Iab-b of the secondary component of system 1:31, since the trigonometric parallax of this star (13.85 ± 2.46 s) is in good agreement with a main sequence (MS) star, but certainly not with a supergiant star. When both components are nearly identical, we assume that they are dwarfs when the giant luminosity class would lead to a tangential velocity larger than 100 km s^{-1}. Thanks to these assumptions, it was possible to assign a mass, but also a distance, to all stars.

We select finally 80 WBs, which are listed in Table 3. In this table, the component A is the same as in H86; therefore, it is usually the brightest one, but with a few exceptions. ϖ is the trigonometric parallax of the system when it was measured for at least one component. When it was measured for both, the mean value is given. The distance D was derived from the trigonometric parallax when its accuracy is better than 20 per cent; otherwise, it was derived from the spectroscopic parallax. The separation between the components was converted to the projected separation, s, in astronomical units. The flag in the last column is assigned in ascending order. It is 1 when the system is a member of an open cluster, otherwise it is 2 when the components of the system are not MS stars later than F5. Otherwise, it is 3 when the components are both fainter than $m_{\rm pg} = 9.1$ mag. Lastly, it is 4 for one system (2:49), which is in fact a faint extension of another one (2:48). Therefore, a blank flag indicates a field WB system of late-type MS stars with at least one component brighter than the completeness limit of AGK2/3. The allotment process of these flags is described in Section 4.1.

The 39 remaining pairs are considered as optical, and their CPM identifications are listed in Table 4.

The distribution of the difference of RVs of the components is shown in Fig. 1. It is worth noticing that we count eight optical pairs among the stars with a RV difference between 2 and 10 km s^{-1}, i.e. one pair per km s^{-1}. Among the pairs with RV difference less than 2 km s^{-1}, we count exactly two optical pairs, i.e. again one pair per km s^{-1}, although their detection comes from the parallaxes only. This indicates that very few optical pairs, if any, were misclassified as physical binaries.

4 THE BIAS-CONTROLLED SAMPLE OF MS WIDE BINARIES

The statistical properties of WBs can be derived only when the selection effects are properly taken into account. This requires a sample that is as complete as possible, and for which the probability detection can be estimated. The WBs listed in Table 3 do not satisfy these two conditions: the selection effects cannot be estimated for all of them, and they are not a complete sample, since we did not observe many close pairs of list 1. Therefore, only a part of them are selected in Section 4.1, and a supplementary list of WBs is added in Section 4.2.

4.1 The bias-controlled sample of CORAVEL MS WBs

First, we reject the systems that probably belong to open clusters. For them, that the components have the same proper motion, the same radial velocity and the same parallax does not mean that they are very probably orbiting binaries. We search the systems that are as close as 10° around the centres of the four most important clusters of the Northern hemisphere, which are the Hyades, the Pleiades, Praesepe and Coma. When the mean RV of a system is that of the cluster, *plus* or *minus* 10 km s^{-1}, we checked if it is a known member. Five systems are, thus, selected: 2:36 belongs to the Hyades, and 1:156, 2:73, 2:74 and 1:175 belong to the Coma cluster. They are indicated by the flag 1 in Table 3.

The method used to derive the intrinsic distribution of the projected separations, in Section 5, assumes that the probability distribution of the apparent magnitude of the secondary component is known. When the primary component is a late-type giant or a supergiant star, this function is hazardous to derive, since it depends on the age of the binary system and on the evolution of both components. Therefore, we decide to consider only systems of components close to the MS, according to the procedure applied in Section 3. We also reject the binaries with a primary component earlier than F5. These early-type stars are difficult to observe with CORAVEL, and it was not possible to observe all of them. The systems rejected because of spectral type or luminosity class are indicated with the flag 2 (except when they are already flagged 1).

We have a problem with the pairs of components where both are fainter than the photographic magnitude $m_{\rm pg} = 9.1$ mag in the AGK2/3 catalogue. Below this value, the density of stars as a function of $m_{\rm pg}$ is fitted well with the following equation:

$$f(m_{\rm pg}) = 3.084 \mathrm{e}^{1.068 m_{\rm pg}} \qquad (2)$$

but the completeness factor drops sharply beyond, as shown in Fig. 2. The completeness factor is defined as the ratio between the number of stars counted in a 0.1-mag bin, and the number predicted by equation (2). For magnitudes brighter than 9.1, the completeness factor is 1, with a variance due to the number of stars per bin. For magnitudes fainter than 9.1, the completeness factor is decreasing, as is the probability that the star is in AGK2/3. It is tempting to assume that the probability of including a pair of stars fainter than 9.1 mag is the product of the completeness factors of both components; unfortunately, this is wrong, since the detection probabilities of two stars recorded on the same photographic plate are correlated. For that reason, the WBs with both components fainter than 9.1 mag are discarded, and they receive the flag 3. For the remaining WBs, the completeness factor of the component fainter than 9.1 mag is the probability of including the pair in AGK2/3.

We also discard the pair 2:49 (flag 4), since its primary component is also that of 2:48. To consider only WBs, but not wide triple systems, we keep the pair with the brightest secondary component.

In the end, we keep only 47 binaries with RVs observed with CORAVEL. These stars are indicated with a blank flag in Table 3.

[1] http://simbad.u-strasbg.fr/simbad/

Table 3. The 80 WBs detected with CORAVEL radial velocities. The flag f indicates the systems rejected from the bias-controlled sample of MS binaries; it is 1 when the system belongs to an open cluster, 2 when the primary component is earlier than F5 or far from the MS, 3 when the components are both fainter than $m_{pg} = 9.1$ mag and 4 when the system contains the faintest component of a triple CPM system.

CPM	AG(A)	V_A (mag)	$B_A - V_A$ (mag)	SpT(A)	AG(B)	V_B (mag)	$B_B - V_B$ (mag)	SpT(B)	$RV_A - RV_B$ (km s^{-1})	ϖ (mas)	D (pc)	s (au)	f
2: 1	+17 8	7.45	0.56	F8	+17 9	8.58	0.93	K0	− 0.30 ± 0.23	26.93 ± 0.51	37	21 296	–
2: 4	+33 51	5.88	1.13	K1III	+33 52	9.28	0.61	F8	− 0.71 ± 0.36	8.61 ± 0.36	116	6536	2
2: 7	+31 55	8.78	0.88	G5	+31 54	9.44	1.04	G5	− 0.01 ± 0.18	–	61	3343	3
1: 9	+12 88	8.91	0.54	F8	+12 89	9.18	0.62	G0	− 0.40 ± 0.33	7.66 ± 0.82	131	5789	–
2: 8	−01 87	9.16	0.53	F7V	−01 90	10.11	0.92	G5	− 2.10 ± 0.62	–	98	9643	3
1: 17	+11 131	8.32	0.58	F8	+11 132	10.22	0.68	K0	− 0.93 ± 0.33	10.56 ± 0.66	95	5148	–
1: 18	+31 132	7.98	0.73	G0	+31 130	8.02	0.61	F8	− 0.54 ± 0.13	16.19 ± 0.58	62	3532	–
2: 9	+37 140	7.52	0.53	F8	+37 138	8.95	0.76	K0	− 0.35 ± 0.25	18.71 ± 0.64	53	13 747	–
1: 20	+60 173	8.55	0.52	F6V	+60 175	9.07	0.52	F6V	− 0.11 ± 0.33	–	100	4437	–
1: 27	+30 199	7.74	0.47	F5	+30 198	9.92	0.71	G0	− 0.79 ± 0.38	11.62 ± 1.01	86	5668	–
1: 31	+58 244	8.07	0.42	F5	+58 243	9.94	0.71	M0Iab-b[a]	− 1.25 ± 0.31	11.17 ± 1.11	90	5103	–
2: 21	+20 280	6.40	1.26	K2	+20 279	8.72	0.46	F5	1.75 ± 2.72	6.64 ± 0.51	151	18 365	2
2: 22	+38 399	7.92	0.39	F0	+38 398	9.72	0.66	G0	− 0.09 ± 0.30	12.20 ± 0.75	82	11 189	2
2: 33	+63 319	8.30	0.79	G7V	+63 318	9.86	1.04	K2V	− 0.96 ± 0.23	15.93 ± 0.67	63	13 167	–
2: 36	+16 384	4.77	0.18	A6IV	+16 385	6.51	0.41	F2	6.61 ± 4.91	23.50 ± 0.25	43	10 637	1
2: 38	+18 367	7.12	0.67	G5	+18 369	9.86	1.18	K7	− 0.38 ± 0.20	22.81 ± 0.82	44	6227	–
2: 40	+29 536	6.66	0.52	F8V	+29 534	8.40	0.74	G0	− 0.19 ± 0.24	18.84 ± 0.58	53	3649	–
2: 41	+27 482	6.96	0.48	F8V	+27 481	9.25	0.94	G5	− 0.64 ± 0.14	25.05 ± 0.67	40	12 572	–
2: 42	+26 477	9.26	1.57	K5	+26 478	9.11	1.39	G5	− 0.40 ± 0.27	4.33 ± 1.14	46	3643	2
2: 44	+44 623	6.73	0.56	F8	+44 621	9.10	0.94	–	− 0.11 ± 0.28	30.20 ± 0.44	33	6361	–
1: 82	+15 742	7.72	0.64	G0V	+15 743	7.72	0.53	F8	− 0.23 ± 0.36	21.62 ± 0.58	46	7958	–
2: 48	+13 732	7.31	0.45	F5	+13 734	7.98	0.54	F8	1.40 ± 0.15	21.64 ± 0.65	46	5149	–
2: 49	+13 734	7.31	0.45	F5	+13 733	9.21	0.94	G5	0.56 ± 0.19	22.02 ± 0.96	45	5075	4
1: 90	+47 746	8.48	0.50	F7V	+47 747	9.77	0.70	G7V	− 0.59 ± 0.96	12.03 ± 1.69	83	3175	–
1: 91	+57 696	7.56	0.42	F2	+57 695	9.27	0.58	–	− 0.50 ± 0.26	14.24 ± 0.61	70	4083	2
1: 93	+32 859	8.35	0.66	G5	+32 858	9.25	0.71	K2	− 1.33 ± 0.15	17.30 ± 1.77	58	6206	–
1:106	+27 979	8.27	0.53	G0V	+27 978	8.26	0.50	G0V	0.15 ± 0.31	22.51 ± 0.85	44	2273	–
2: 55	+51 744	6.11	0.42	F3V	+51 745	7.80	0.74	G5	− 1.24 ± 0.16	36.08 ± 0.41	28	6399	2
1:112	−02 517	4.60	0.46	F5V	−02 518	7.15	0.87	K0	− 1.16 ± 0.20	57.69 ± 2.14	17	1137	–
1:114	+14 1033	9.01	0.72	G5	+14 1032	8.74	0.64	G0	− 0.19 ± 0.14	–	62	5094	–
2: 56	−00 1459	6.71	1.06	K0III	−00 1460	10.50	0.67	K	− 0.34 ± 0.31	9.06 ± 0.52	110	12 061	2
2: 57	+33 1010	7.98	0.47	F8	+33 1011	8.72	0.54	G	− 0.70 ± 0.32	11.35 ± 0.70	88	18 122	–
2: 58	+21 1119	8.80	0.38	F8	+21 1120	9.15	0.40	F8	0.37 ± 0.39	4.80 ± 0.85	208	40 785	–
1:127	+56 797	4.83	0.49	F8V	+56 796	8.76	1.34	M0	− 0.26 ± 0.13	78.26 ± 0.28	13	1569	–
1:130	+46 852	5.20	0.31	F5III	+46 854	7.28	0.58	F9V	0.87 ± 5.34	26.93 ± 0.23	37	10 671	–
1:140	+43 1013	7.18	0.53	F8	+43 1012	8.24	0.60	G5	− 1.57 ± 0.27	21.12 ± 0.47	47	6384	–
1:141	+02 1472	8.32	1.02	K0/1III	+02 1473	10.21	0.50	F7V	− 0.55 ± 0.16	4.55 ± 0.90	220	14 048	2
2: 65	+41 1063	8.05	0.47	F8	+41 1064	9.10	0.65	G	− 0.02 ± 0.25	12.54 ± 1.15	80	10 671	–
1:156	+20 1296	4.54	0.52	A7V+...	+20 1295	8.96	0.59	G5	− 2.11 ± 1.02	14.02 ± 0.23	71	5315	1
1:158	+09 1459	7.34	0.96	K0	+09 1458	7.87	0.47	K0III-IV	− 0.26 ± 0.18	10.25 ± 0.53	98	3031	2
2: 66	+63 648	9.21	0.59	G	+63 650	10.03	0.76	G5	1.12 ± 0.31	–	92	13 421	3
2: 70	+36 1135	8.10	0.46	F8V	+36 1139	8.20	0.38	F3	− 0.12 ± 0.19	9.33 ± 0.93	107	25 734	–
2: 71	+73 326	9.79	0.71	G0	+73 327	10.03	0.65	F8	− 0.23 ± 0.39	–	116	9018	3
2: 73	+20 1355	8.43	0.79	K0V	+20 1356	8.80	0.95	K3V	0.05 ± 0.13	–	30	12 354	1
2: 74	+25 1366	9.10	0.87	K0IV	+25 1369	9.92	1.20	K5IV-V	− 0.06 ± 0.16	26.63 ± 0.97	38	13 993	1
1:175	+21 1322	4.91	0.89	G5III	+21 1323	9.36	0.83	–	− 1.38 ± 0.16	11.52 ± 0.87	87	2456	1
2: 76	+67 574	6.52	1.15	K2III	+67 570	6.96	1.15	K2III	− 0.41 ± 0.18	8.58 ± 0.27	117	20 855	2
1:190	+10 1635	6.49	1.04	K0III	+10 1636	8.97	0.44	F6V	− 0.50 ± 0.24	8.38 ± 0.49	119	8364	2
1:194	+38 1289	5.51	1.04	K0III	+38 1288	8.86	0.53	F8V	− 0.67 ± 0.23	10.29 ± 0.33	97	6950	2
1:196	+26 1388	6.95	0.44	F6V	+26 1389	8.83	0.77	K0	− 0.12 ± 0.27	22.72 ± 0.50	44	4269	–
2: 88	+30 1364	7.69	0.62	G0	+30 1366	7.95	0.62	G2IV	− 0.19 ± 0.19	18.93 ± 0.50	53	16 088	–
2: 89	+83 385	9.55	0.60	K0	+83 383	10.71	0.70	F8	− 3.54 ± 2.66	1.00 ± 11.00	136	8117	2
1:216	+33 1351	3.49	0.95	G8IV	+33 1352	7.81	0.58	G0Vv	− 0.59 ± 0.20	26.79 ± 0.16	37	3913	2
1:237	+08 1965	6.97	0.88	G5	+08 1966	8.26	0.55	G5	0.18 ± 0.19	13.32 ± 0.54	75	4414	2
2: 91	+69 664	8.01	0.26	F0	+69 663	8.00	0.40	F5	3.17 ± 5.56	9.03 ± 0.48	111	16 267	2
1:241	+06 1960	6.58	0.88	G5	+06 1958	10.30	1.04	K3	0.25 ± 0.32	21.94 ± 0.57	46	7427	–
2: 92	+05 2201	9.73	0.84	G5	+05 2202	10.90	0.52	F8	0.18 ± 0.29	–	98	5800	3
1:242	+47 1214	7.88	1.04	K3V	+47 1216	7.83	0.98	K3V	− 0.50 ± 0.12	55.54 ± 0.39	18	2033	–
1:246	+86 233	8.35	0.39	F2	+86 232	9.20	0.50	G0	0.01 ± 0.22	8.73 ± 0.49	115	3578	2
2: 94	+46 1275	8.27	0.50	F5	+46 1274	10.28	0.78	G5	− 0.22 ± 0.18	–	100	19 920	–
2: 95	+63 904	7.67	0.52	F9V	+63 903	8.39	0.73	G0	− 0.17 ± 0.21	22.12 ± 0.36	45	8750	–

Table 3 – *continued*

CPM	AG(A)	V_A (mag)	$B_A - V_A$ (mag)	SpT(A)	AG(B)	V_B (mag)	$B_B - V_B$ (mag)	SpT(B)	$RV_A - RV_B$ (km s^{-1})	ϖ (mas)	D (pc)	s (au)	f
1:258	+28 1759	8.10	0.52	F8	+28 1761	8.22	0.53	F8	0.19 ± 0.13	12.46 ± 0.61	80	4472	–
1:261	+45 1487	8.33	0.48	F8IV	+45 1486	9.29	0.51	G0.5IV	− 0.75 ± 0.29	9.48 ± 0.67	105	3100	–
2:100	+03 2375	8.30	0.42	F2/3V	+03 2377	9.16	0.49	G0	− 0.61 ± 0.31	–	87	7649	2
1:264	+34 1826	7.25	0.45	F5	+34 1825	10.16	0.94	K0	− 3.46 ± 0.81	15.02 ± 0.50	67	2191	–
1:280	−02 1185	6.70	0.47	F7V	−02 1184	7.48	0.48	F6V	0.11 ± 0.13	21.58 ± 0.41	46	2763	–
2:103	+17 2205	9.04	0.49	G0	+17 2206	9.79	0.59	G0	0.34 ± 0.37	–	92	11 631	3
1:282	+14 2238	8.59	0.43	G0	+14 2237	10.26	0.43	G5	− 1.42 ± 0.29	8.10 ± 0.96	123	9234	–
1:283	+80 431	5.96	0.92	K0III+..	+80 432	8.66	0.59	G5	− 0.45 ± 0.23	15.48 ± 0.21	65	13 832	2
1:284	+32 1986	8.17	0.53	F6V	+32 1987	8.69	0.62	F9V	− 1.04 ± 0.34	–	73	3908	–
2:106	+41 2028	6.60	0.91	G0	+41 2027	8.81	0.58	G0	− 0.34 ± 0.31	14.83 ± 0.38	67	31 003	–
2:107	+57 1428	8.13	0.54	G5	+57 1427	8.63	0.53	K0	0.22 ± 0.25	10.56 ± 0.69	95	7951	–
1:300	+18 2249	8.48	0.44	F8	+18 2248	10.46	0.44	G5	− 0.78 ± 0.23	–	129	8494	–
1:307	+72 613	7.58	0.39	F5	+72 614	8.41	0.42	F5	− 1.27 ± 0.44	11.81 ± 0.44	85	3616	–
2:110	+29 2849	8.47	0.38	F5V	+29 2850	10.38	0.67	K0	0.03 ± 0.36	8.40 ± 1.00	119	20 744	–
1:310	+67 1041	6.98	0.42	F2	+67 1040	7.52	0.46	F5	− 0.72 ± 0.61	16.81 ± 0.28	59	4129	2
2:111	+45 2142	8.49	0.64	G5	+45 2141	7.88	0.57	G0	− 0.21 ± 0.22	17.63 ± 0.70	57	10 503	–
2:112	+59 1650	9.70	0.58	K0	+59 1651	9.56	0.60	G0	− 0.21 ± 0.30	–	93	10 202	3
2:113	+40 2513	7.71	0.58	G0	+40 2512	8.15	0.64	G0	0.66 ± 0.27	23.21 ± 0.46	43	4948	–
1:326	+10 3290	8.73	0.62	G0	+10 3289	8.50	0.55	F8	− 0.65 ± 0.27	12.18 ± 0.65	82	5212	–

[a]The luminosity class is ignored, since it does not match the magnitude and the trigonometric parallax of the star; see explanations in the text.

Table 4. The 39 optical pairs with CORAVEL radial velocities for both components. Two of them (2:87 and 2:99) are detected by the Hipparcos trigonometric parallaxes of the components.

CPM	CPM	CPM	CPM	CPM	CPM	CPM	CPM
2:3	2:5	2:6	1:19	2:10	2:13	2:14	2:15
2:16	2:17	2:18	2:19	2:46	2:53	2:54	2:59
2:62	2:63	2:64	2:67	2:68	2:72	2:75	2:78
2:80	2:81	2:82	2:83	1:195	2:84	2:85	2:87
2:90	2:93	2:99	2:101	2:105	2:108	2:109	

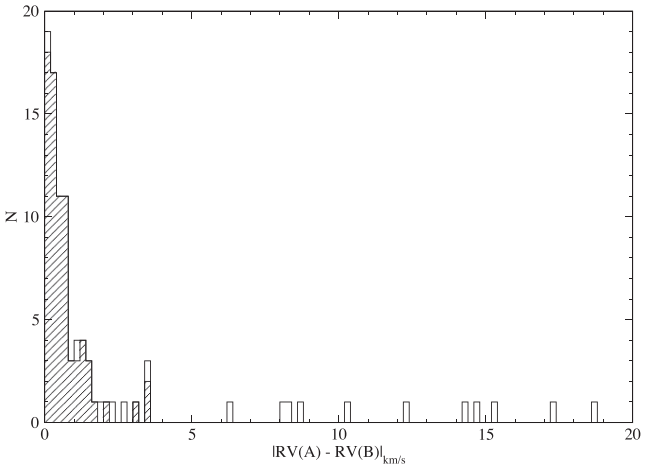

Figure 1. Histogram of the differences of radial velocities for the 119 CPM pairs with both components observed with CORAVEL. The hatched area refers to the WBs in Table 3.

4.2 The supplementary list of MS WBs

Many pairs in the lists of H86 were not observed with CORAVEL since their probability of being gravitationally bound is very high. This applies to the pairs of list 1 with $T < 350$ yr, and a few others for which the RVs were already well known. These systems must be taken into account when their primary component is at least as bright as $m_{pg} = 9.1$ mag and at least as late as F5, and when the components seems to be close to the MS. They are selected as explained below.

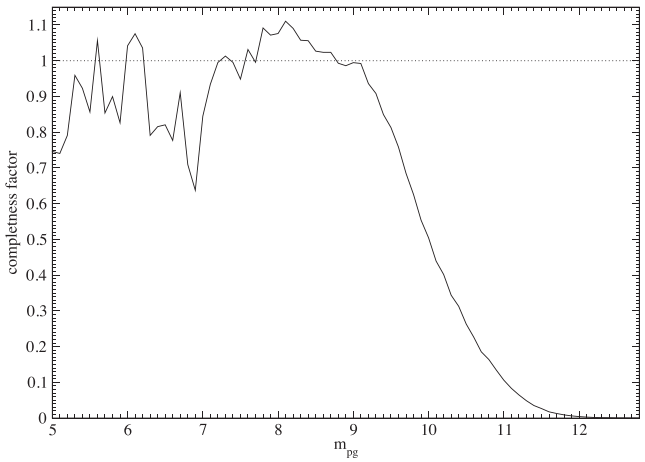

Figure 2. The completeness factor of AGK2/3 as a function of the photographic magnitude, when the distribution in equation (2) is assumed. For $m_{pg} \leq 9.1$ mag, the deviations from unity are ignored.

First, the same selection criteria as for the systems observed with CORAVEL are applied. The status of the pair 1:213 is puzzling. On one hand, the components have incompatible parallaxes in Hipparcos 2 (van Leeuwen 2007). On the other hand, the parallaxes were compatible in the first Hipparcos reduction, T is only 40 yr, the spectral type of the secondary component matches the absolute magnitude derived from the first Hipparcos reduction much better than that derived from Hipparcos 2, and, above all, the difference in the RVs of the components, obtained from Simbad, is only (0.06 ± 0.11) km s^{-1}. Therefore, we finally decided to consider this pair as a physical binary.

One more selection criterion must still be added: by including the pairs with $T < 350$ yr, we include the pairs with separations close to the resolving power of the instrumentation used to prepare the

Table 5. The 12 WBs rejected from the MS bias-controlled sample because the components are so close that similar systems could have been undetected.

CPM	CPM	CPM	CPM	CPM	CPM
1:65	1:69	1:84	1:95	1:129	1:146
1:202	1:208	1:265	1:288	1:293	1:320

AGK2/3 catalogue. Therefore, some close pairs may be included in our list by chance, although they are so close that the probability of detecting the secondary component was small. This may induce a selection effect that will be hazardous to correct. For safety, we prefer to discard the pairs that are too close to be sure that their detection was complete. We assume that the components of a close pair are certainly both in AGK2/3 when the separation is larger than the sum of overestimations of the images of the components derived in the Appendix, equation (A2). This results in discarding the 12 pairs listed in Table 5. The supplementary list to the controlled-biased sample of MS binaries is, thus, obtained. It is presented in Table 6. As for the CORAVEL pairs, we ignore the luminosity class of a star when it is obviously erroneous. This concerns the two following stars: (1) 1:192B = AG +39 1356, since its proper motion leads to a tangential velocity of about 660 km s^{-1} when the star is assumed to be a giant, and (2) 1:223A = HIP 75676 has the absolute magnitude $M_V = 4.94$ mag according to Hipparcos data. Both are taken as dwarfs instead of giants.

The systems with a blank flag in Table 3 and all those in Table 6 constitute the bias-controlled sample of MS WBs, or, for brevity, the BC sample hereafter. This sample contains 116 systems. The primary components have spectral types between F5 and K3. This range is not much larger than that of the sample studied by Duquennoy & Mayor (1991), which was F7–G9, or by Raghavan et al. (2010), which was F6–K3. The distribution of $\log s$ of the BC sample is presented in Fig. 4.

5 STATISTICAL PROPERTIES OF THE WIDE BINARIES

5.1 The parent population of the BC sample of MS WBs

Our aim is to derive the frequency of MS WBs as a function of the projected separation. We have a sample of MS WBs with known separations, but we must take into account the selection effects. For that purpose, we need to select all the stars in AGK2/3 that could be the primary component of a MS WB of the BC sample. This selection is called the parent population of the MS WBs hereafter.

We apply to the stars of AGK2/3 the same selection criteria as for the primary components of the BC sample, as summarized below:

(i) Proper motion larger than 50 mas yr^{-1}, since the selection of wide pairs in H86 concerned only stars above this limit.

(ii) Photographic magnitude $m_{\rm pg}$ at least as bright as 9.1 mag.

(iii) Position at more than 10° from the centres of the four open clusters considered in Section 4.1.

(iv) Spectral type at least as late as F5. When existing, the spectral type in Simbad is preferred to that in AGK2/3. When the subclass is missing, the $B - V$ colour index is used to estimate it.

(v) Luminosity class close to the MS. The luminosity class is taken from Simbad. When the trigonometric parallax of the star is known, the luminosity class is estimated from the absolute magnitude. Otherwise, the following procedure is applied. The distance of the star is derived, assuming it is a giant. The components (U, V, W) of the spatial velocity of the star are derived from the proper motion, the distance and the motion of the Sun. When one of these components is 3 times larger than the standard deviation provided by Fiala (2000), it is inferred that the star is a dwarf.

A parent population of 6372 stars is, thus, selected for the BC sample. For each star, the spectral type, the mass, the apparent magnitude, the distance and the proper motion are known.

5.2 Weighting the MS WBs of the BC sample

The detection probability of any WB with a given separation is derived from the parent population with a simulation. For each parent star, the mass of a synthetic companion is generated from a mass distribution. When the mass of the companion is larger than that of the parent star, the synthetic companion is ignored, and another one is generated. The magnitude and the $(B - V)$ colour index of the synthetic companion are then derived from its mass and from the distance of the parent star. They are used to calculate the apparent photographic magnitude, thanks to the following equation, which was obtained from the parent population:

$$m_{\rm pg} = m_V + 1.15(B - V). \quad (3)$$

The companion receives a weight equal to its probability of being recorded in AGK2/3 due to its brightness. For a companion brighter than $m_{\rm pg} = 9.15$ mag, the weight is 1. For a faint star, it is the completeness factor in Fig. 2. The weight applies to a companion in the allowed range of separations (the apparent and the projected separations are equivalent, since the distance is known). The closest separation comes from the sum of the radii of the images of the stars, in equation (A2). The maximum separation comes from the proper motion, μ, and from the selection limit of list 2, which was $T = \rho/\mu < 3500$ yr. Between these two limits, the weight of the companion is added to each bin of the overall detection probability of the WBs. This procedure is repeated 10 000 times for each parent star. The overall detection probability as a function of the projected separation is finally normalized to be 1 at its maximum.

The detection probability of the WBs, as derived above, depends on the mass distribution of the companions. In theory, this distribution may be derived from the BC sample, using the method of the nested boxes (Halbwachs 2001; Eggenberger et al. 2004). Unfortunately, the results are not reliable at all, because most of the WBs have secondary components only about 1 mag fainter than the primary component, due to selection effects. Therefore, the BC sample leads to a distribution of mass ratios from 1 to around 0.8 only. We prefer then to choose among theoretical distributions. To investigate the importance of this choice, we tried three different distributions: the constant distribution, the Salpeter distribution $f(\mathcal{M}) \propto \mathcal{M}^{-2.35}$ (Salpeter 1955) and a distribution obtained by random pairing assuming the initial mass function (IMF) found by Kroupa et al. (2013). This IMF is defined as a power law in three parts:

$$\begin{aligned} \psi(\mathcal{M}) &= 0.2410\mathcal{M}^{-1.3},\ \mathcal{M} \in [0.07, 0.5], \\ \psi(\mathcal{M}) &= 0.1205\mathcal{M}^{-2.3},\ \mathcal{M} \in [0.5, 1], \\ \psi(\mathcal{M}) &= 0.1205\mathcal{M}^{-2.7},\ \mathcal{M} \in [1, 10]. \end{aligned} \quad (4)$$

The resulting probability distributions are presented in Fig. 3. Surprisingly, the curves obtained from the three mass distributions are very close. In what follows, the random pairing distribution is assumed.

Table 6. The 69 WBs of the supplementary list of the BC sample.

CPM	AG(A)	V_A (mag)	$B_A - V_A$ (mag)	SpT(A)	AG(B)	V_B (mag)	$B_B - V_B$ (mag)	SpT(B)	ρ (arcsec)	ϖ (mas)	σ_ϖ (mas)	D (pc)	s (au)
1:14	+51 118	8.09	0.45	F8	+51 117	8.53	0.49	F8	14.6	13.06	3.19	66	970
1:29	−00 223	6.87	0.62	G2V	−00 222	10.52	1.23	K5	79.0	27.06	0.58	37	2919
1:32	+28 257	7.00	0.49	F5V	+28 256	7.74	0.59	G2V	14.4	30.46	2.58	33	473
1:34	+34 226	7.75	0.58	G0IV	+34 227	9.40	0.60	F8	10.2	11.14	1.30	90	917
1:35	+15 205	8.88	0.63	G5	+15 204	9.38	0.69	G5	34.7	17.20	1.04	58	2015
1:38	+55 259	6.95	0.48	F5V	+55 258	9.58	0.77	K2V	21.1	18.28	0.69	55	1154
1:39	+24 227	6.48	0.38	F6III	+24 226	7.09	0.50	F4V	37.9	24.19	0.45	41	1567
1:43	+38 324	5.36	0.37	F6V	+38 323	9.68	0.78	–	14.2	14.15	0.72	71	1004
1:47	+07 353	7.37	0.59	F8	+07 354	7.75	0.63	G0	156.0	22.50	0.73	44	6933
1:51	+63 274	6.80	0.46	F5	+63 275	8.20	0.83	G5	45.8	23.73	0.47	42	1931
1:53	+41 396	8.78	0.15	K1V	+41 397	8.78	0.88	K2V	7.4	45.65	2.63	22	162
1:64	+07 535	8.38	0.89	K0	+07 536	8.20	0.83	K0	16.4	33.00	4.00	30	496
1:66	+63 355	7.60	0.67	G0	+63 354	7.90	0.74	G0	32.5	31.03	0.61	32	1048
2:43	+17 485	5.00	0.52	F8V	+17 482	7.92	1.13	K4V	707.2	69.62	0.37	14	10 158
1:70	+54 477	7.53	0.64	G1V	+54 476	9.71	1.00	K3:	8.4	25.44	1.04	39	329
1:72	+53 486	6.23	0.84	K1V	+53 487	9.87	1.44	M0.5	98.0	81.35	0.51	12	1204
1:75	−00 757	8.74	0.61	G5	−00 758	10.07	0.93	–	9.2	–	–	51	468
1:80	+75 308	7.12	0.56	G0	+75 309	8.24	0.75	G5	12.6	28.29	1.41	35	446
1:83	+22 841	8.03	0.50	F5	+22 842	8.33	0.46	F5	8.7	6.11	1.39	82	719
1:85	+03 1049	7.02	0.51	F8	+03 1050	10.27	0.97	–	10.0	19.63	0.70	51	509
1:92	+45 762	7.70	0.61	G0V	+45 761	9.17	0.92	K0V	29.0	26.43	1.15	38	1097
1:94	−00 1234	9.14	0.57	G0	−00 1235	10.03	0.74	–	39.5	13.83	1.47	72	2855
1:96	+05 1272	7.25	0.59	G1V	+05 1273	8.41	0.80	G5	26.3	28.10	0.92	36	936
1:104	+03 1253	8.43	0.45	F5	+03 1252	8.31	0.54	F5	11.7	9.82	2.44	90	1051
1:113	+10 1224	8.85	0.92	G9V	+10 1223	8.76	0.86	G5	14.0	38.97	6.84	26	360
1:116	+10 1276	8.09	1.13	G5	+10 1275	10.44	0.96	G0	18.4	7.16	1.68	75	1373
1:117	+20 1142	7.60	0.56	G0	+19 1017	8.40	0.70	G5	30.4	23.91	0.59	42	1271
1:118	+06 1268	7.64	0.44	F5	+06 1269	10.53	0.97	F5	23.4	16.66	0.67	60	1404
1:131	+13 1081	9.38	0.48	F8	+13 1080	8.80	0.60	F8	17.5	10.12	11.59	95	1665
1:138	+07 1509	8.70	0.44	F8	+07 1510	10.15	0.75	G3V	7.8	9.15	1.56	109	848
1:142	+53 801	6.50	0.41	F6V+...	+53 800	7.95	0.58	F2	12.9	28.29	1.00	35	456
1:145	+03 1496	6.49	0.80	K0IV	+03 1497	7.53	1.02	K2V	28.3	56.21	0.67	18	504
1:148	+14 1209	6.20	0.57	G0V	+14 1208	9.22	1.14	G5	15.6	42.32	1.20	24	370
1:155	+11 1358	8.91	0.53	G5	+11 1357	11.30	0.90	G5	8.7	10.30	1.55	97	846
1:161	+19 1174	8.22	0.71	G6V	+19 1175	8.43	0.76	G5	73.7	25.20	0.84	40	2922
1:164	+55 818	7.82	0.49	F8	+55 819	8.35	0.57	F8	22.0	19.42	1.58	51	1134
1:165	+53 844	8.03	0.88	K0V+K1v.	+53 843	8.18	0.86	K0	12.7	30.61	2.13	33	415
1:167	+09 1498	7.48	0.62	G0	+09 1497	9.64	0.98	K2	23.4	18.04	0.85	55	1298
1:182	+24 1359	8.16	0.68	G9V	+24 1360	8.59	0.76	K0V	39.0	27.74	0.74	36	1407
1:184	−02 789	7.68	0.51	F8	−02 788	10.02	0.65	–	8.9	18.03	0.94	55	491
1:186	+02 1666	7.06	0.77	G5	+02 1667	7.36	0.82	G5	26.7	63.35	0.94	16	421
1:192	+39 1357	7.78	0.67	G5V	+39 1356	9.15	0.92	K1III[a]	56.2	21.74	0.80	46	2585
1:203	+48 1134	7.63	0.41	F5	+48 1133	9.40	0.49	F5	19.7	11.07	1.12	90	1778
1:213	+19 1419	6.68	0.68	G5V	+19 1420	7.53	0.73	G7V	23.7	34.20	1.78	29	694
1:215	+62 862	8.04	0.50	F7V	+62 861	8.74	0.65	B0	15.8	13.92	2.50	72	1132
1:218	+10 1798	7.13	0.49	F8V	+10 1799	8.01	0.58	G5	13.1	23.00	3.82	43	571
1:223	+43 1277	7.47	0.67	G2III[b]	+43 1276	9.62	1.06	K	40.0	31.12	0.59	32	1286
1:224	+80 347	6.58	0.67	G0IV-Vv+	+80 348	7.31	0.79	G5	31.3	46.03	0.29	22	680
1:225	+39 1516	6.77	0.91	K2V	+39 1515	7.56	0.97	K3V	121.8	44.76	0.42	22	2721
1:227	+36 1363	7.80	0.43	F5	+36 1364	7.40	1.10	F5	14.8	7.17	5.36	63	931
1:229	+36 1372	7.57	0.48	F5	+36 1371	8.73	0.56	–	30.0	12.73	0.55	79	2357
1:236	+46 1174	7.91	0.80	G5	+46 1173	10.06	0.75	G5	93.7	11.95	0.51	84	7840
1:247	+31 1517	8.50	0.59	G1V	+31 1516	9.57	0.73	G8V	68.0	14.37	0.69	70	4733
1:248	+04 2132	8.70	0.60	G5	+04 2131	10.90	0.80	–	24.5	–	–	50	1227
1:253	+27 1677	3.41	0.76	G5IV	+27 1676	10.8	0.45	–	33.0	120.33	0.16	8	275
1:255	+03 2184	7.87	0.43	F5	+03 2183	10.18	0.82	–	9.0	–	–	71	644
1:257	+79 491	5.68	0.46	K2Vv	+79 490	6.02	0.47	F7	19.0	15.26	3.06	17	328
1:262	+06 2406	6.92	0.43	F5	+06 2407	9.10	0.50	–	9.8	15.17	0.82	66	643
1:266	+50 1407	5.96	0.64	G1.5Vb	+50 1408	6.20	0.66	G3V	39.0	47.29	0.19	21	824
1:267	+33 1831	4.99	0.47	F7V	+33 1832	8.56	1.04	K6V:	25.8	47.10	0.26	21	547
1:272	+20 2208	6.49	0.36	F5IV	+20 2207	8.78	0.70	F2	11.2	22.25	0.64	45	502
1:273	+57 1348	8.67	0.43	F8	+57 1349	9.89	0.74	–	8.0	–	–	78	624
1:275	+06 2688	7.70	0.67	G4IV	+06 2687	8.02	0.64	G4V	42.9	16.32	0.92	61	2627

Table 6 – *continued*

CPM	AG(A)	V_A (mag)	$B_A - V_A$ (mag)	SpT(A)	AG(B)	V_B (mag)	$B_B - V_B$ (mag)	SpT(B)	ρ (arcsec)	ϖ (mas)	σ_ϖ (mas)	D (pc)	s (au)
1:296	+57 1471	7.40	0.46	F5V	+57 1472	8.76	0.62	–	12.6	–	–	58	726
1:298	+82 650	6.98	0.45	F6IV-V	+82 651	7.43	0.63	F5	13.4	33.47	2.12	30	401
1:306	+56 1594	7.62	0.65	G0	+56 1595	9.67	0.79	–	17.0	–	–	40	684
1:314	+47 2022	7.14	0.61	G5	+47 2021	7.93	0.88	G5Ve	15.1	40.59	1.88	25	373
1:321	+05 3406	7.73	0.59	F8	+05 3405	8.50	0.73	F8	15.0	–	–	61	908
1:324	+24 2585	7.87	0.61	G5	+24 2584	9.41	0.71	G0	9.4	30.00	7.00	56	524

[a]The luminosity class is ignored, since it does not match the magnitude and the proper motion of the star; see explanations in the text. [b]The luminosity class is ignored, since it does not match the magnitude and the trigonometric parallax of the star; see explanations in the text.

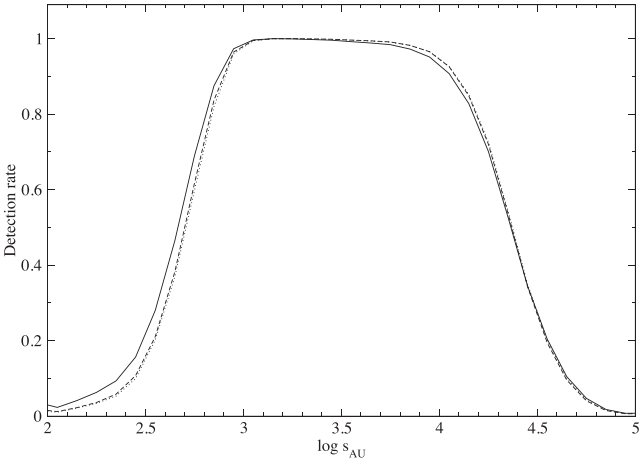

Figure 3. The probability of detecting a BC sample binary, as a function of the projected separation. Three different distributions are assumed for the mass of the companion: dotted line: constant distribution; dashed line: Salpeter distribution; full line: random pairing from the IMF. To facilitate comparisons, the maximum probability of each distribution is arbitrarily set to 1.

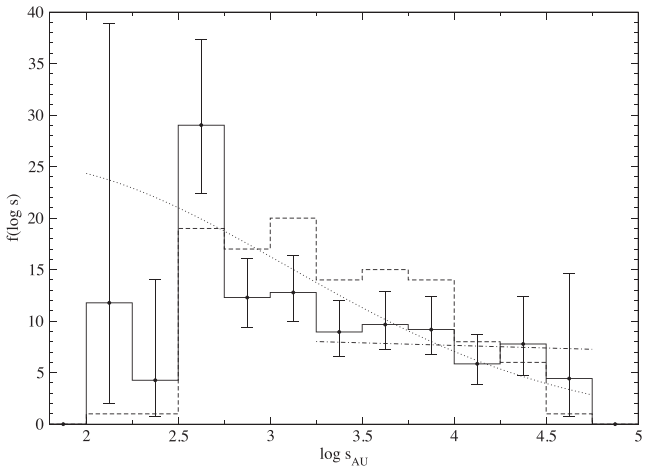

Figure 4. The distribution of the projected separations of the MS WBs. The dashed line is the count of the systems in the BC sample. The full line is the distribution corrected for selection effects. The dotted line is the log-normal distribution derived from the parameters of Raghavan et al. (2010), normalized on $\log s$ between 2.5 and 4.5. The dashes and dots correspond to the power law distribution $f(a) \propto a^{-1.5}$, for $\log s > 3.25$. The error bars are derived from the limits of the counts, assuming they obey a Poisson distribution.

5.3 The intrinsic distribution of projected separations

It is now possible to derive the intrinsic distribution of the projected separations of the MS WBs. For each of the 116 systems of the BC sample, we obtain a probability from Fig. 3. We assign to the system a weight that is the inverse of the probability, and we build the intrinsic distribution of $\log s$ by adding the weights instead of counting the systems. The resulting distribution is shown in Fig. 4. To help the comparison, it is normalized to obtain the number of WBs in the BC sample. The error bars are derived from the Poisson distribution. The upper and the lower limits correspond to the rate parameter providing the actual count or less with a 84 per cent probability, or with a 16 per cent probability, respectively.

It appears that the intrinsic distribution of $\log s$ is rather flat for $\log s$ between 2.75 and 4.5, i.e. from about 600 to 30 000 au.

We compare our distribution with three distributions frequently found in previous studies, which are the constant distribution, the power law distribution and the log-normal distribution. The constant distribution of $\log s$ was first found by Öpik (1924), and it was recently obtained by Longhitano & Binggeli (2010) for WBs, when Lépine & Bongiorno (2007) accepted it only until $s = 4000$ au. The Kolmogorov test is used for the comparison. The cumulative distribution function of each $\log s$ in our sample is derived, taking into account the probability detections in Fig. 3. Since the number of WBs in our sample, $N_{\rm WB}$, is sufficiently large, we consider the product $d_{\rm K}\sqrt{N_{\rm WB}}$, where $d_{\rm K}$ is the maximum distance between the cumulative distribution of $\log s$ for our sample, and that corresponding to Öpik's law and to the probability detection. We find $d_{\rm K}\sqrt{N_{\rm WB}} = 1.77$. The probability of getting such a large distance is only 0.3 per cent, leading to the conclusion that the constant distribution is inconsistent with our data.

The power law distribution $f(a) \propto a^{-\lambda}$ was found by Wasserman & Weinberg (1991) and more recently by Tokovinin & Lépine (2012) for a larger than 2000 au, with $\lambda = 1.5$. The latter distribution is in very good agreement with our sample for $\log s > 3.25$, since the Kolmogorov test gives $d_{\rm K}\sqrt{N_{\rm WB}} = 0.7121$, leading to a 66 per cent probability.

The log-normal distribution was proposed by Kuiper (1935). Its parameters were accurately derived by Duquennoy & Mayor (1991), and slightly ameliorated by Raghavan et al. (2010). From a sample including 87 WBs with periods longer than 1 000 000 d, i.e. in the same range of separation as our present sample, they obtained a log-normal distribution around the mean $\overline{\log P} = 5.03$ when P is expressed in days, and with the standard deviation $\sigma_{\log P} = 2.28$. Since their study focused on solar-type stars, their distribution of $\log P$ is easily converted to a distribution of semi-major axes, a. Assuming that the total mass of each system is around 1.5 solar masses, one obtains another log-normal distribution, around $\overline{\log a} = 1.70$ (a in astronomical units), with $\sigma_{\log a} = 1.52$. Assuming, like

them, that $\log s = \log a - 0.13$, the distribution of $\log s$ is log-normal with the same standard deviation, but around $\overline{\log s} = 1.57$. This distribution is drawn on Fig. 4. The Kolmogorov test is used again to check the compatibility of this distribution with our sample. We find $d_K\sqrt{N_{WB}} = 0.928$. The probability of obtaining this distance or even more is 34 per cent. Therefore, our WBs are in rather good agreement with the log-normal distribution.

6 THE MULTIPLE SYSTEMS

6.1 The sample

33 WBs have at least one SB component, and the systems in Table 3 include a total of 37 SBs that were studied in Paper I. The mass ratios of the double-lined SBs (SB2), q, and the logarithms of the periods of the SB orbits are listed in Table 7.

Despite its moderate size, this sample may be used to investigate some properties of multiple systems. So, we will look at the correlation between the periods of WBs and that of SBs, the ratio between the frequencies of quadruple and triple systems and the period distribution of the SBs.

6.2 Frequency of quadruple systems with respect to the triple systems

We want to see if the formation of a close binary is due to peculiar conditions that are common to both components. If this is true, quadruple systems are expected to be more frequent than when we assume that the probability of having a SB is the same for any WB components.

To investigate this question, we consider the WBs for which a SB could be equally detected for both components. We discard the systems belonging to open clusters ($f = 1$), since their selection as WBs is questionable. The systems containing a late-type giant or a star earlier than F5 ($f = 2$) are discarded, because the former correspond to long-period SBs and the latter are difficult to measure with CORAVEL. The detection of SBs with unknown periods or with periods longer than 10 yr is facilitated when the other WB component is also a SB, since both stars were then observed more frequently than the others; for that reason, only WBs with SBs with $P < 10$ yr or $\log P < 3.563$ are considered. The system 2:49 ($f = 4$) is discarded too, since its SB component belongs also to 2:48. After this selection, we count 22 SBs among the 53 systems of Table 3 that do not have $f = 1$, 2 or 4 and that are not rejected because the period of the SB component is longer than 10 yr. The overall SB proportion is then $p_{SB} = 22/(2 \times 53)$. The expected number of triple systems is $n_3 = 53 \times p_{SB} \times (1 - p_{SB}) \times 2 = 17.4$, and the expected number of quadruple systems is $n_4 = 53 \times p_{SB}^2 = 2.3$. These numbers match very well with the actual counts, which are 18 and 2, respectively. That the number of quadruple systems is exactly that expected from independent probabilities firmly supports the hypothesis that the probability of being a close binary with a period shorter than 10 yr is the same for any WB component, regardless of the possible binarity of the other component. In fact, the excess of quadruple systems found by Tokovinin (2014) and Riddle et al. (2015) is due to subsystems with periods longer than 10 yr.

6.3 Properties of the tertiary components

We consider now the 18 triple systems of the previous section to see if the single component of the WB is less massive than the SB, as suggested in the past by Tokovinin (2008). We count 12 SBs as the A component of the WB and six SBs as the B component.

Table 7. The 33 multiple systems among the 80 WBs detected from CORAVEL radial velocities. P_A and P_B are the periods of the components of the WBs when they are SBs. P_{WB} is an estimation of the period of the WBs. The periods are all expressed in days. The flag f is the same as in Table 3. The periods of the SBs considered in Section 6.5 are indicated by an asterisk.

CPM	q_A	$\log P_A$	q_B	$\log P_B$	$\log P_{WB}$	f
2: 7	–	1.399*	–	–	7.85	3
2: 8	–	1.768*	–	?	8.51	3
1: 18	0.996	1.173*	–	–	7.82	–
1: 31	–	3.225*	–	–	8.14	–
2: 21	–	–	–	3.5:	8.88	2
2: 33	–	1.835*	–	3.420*	8.72	–
2: 38	–	–	0.746	1.752*	8.31	–
2: 40	0.620	3.167*	–	–	7.87	–
2: 41	–	–	–	3.357*	8.69	–
2: 48	–	–	–	3.433*	8.00	–
2: 49[a]	–	3.433	–	–	8.10	4
1: 93	0.857	3.176*	–	–	8.25	–
1:112	–	3.449*	–	–	7.09	–
1:114	–	2.584*	–	–	8.11	–
2: 58	–	1.792*	0.624	3.362*	9.38	–
1:130	?	?	–	0.750*	8.47	–
1:141	–	1.938	–	–	8.72	2
2: 65	–	–	–	2.978*	8.55	–
1:156	0.913	1.855	–	>3.6	7.92	1
2: 70	–	3.612	–	–	9.10	–
2: 73	–	–	–	3.462	8.75	1
2: 74	–	–	0.957	1.289	8.82	1
1:175	–	3.464	–	–	7.60	1
2: 89	–	>3.9	–	–	8.68	2
2: 92	–	0.742*	–	–	8.71	3
1:246	–	–	0.643	0.773*	7.83	2
2: 94	–	2.974*	–	–	8.92	–
1:258	–	3.546*	–	–	7.98	–
1:280	0.845	2.206*	–	–	7.64	–
1:300	–	–	0.933	0.968*	8.32	–
1:307	0.566	0.660[b] *	–	–	7.82	–

[a]The WB component 2:49A is also 2:48B.
[b]1:307A is a triple system; we keep only the shortest period. The long period is 50 yr.

However, the A component is sometimes the brightest one because it is a close binary: in Table 3 the spectral types of the B components of the WBs 1:18, 1:114, 2:92 and 1:280 are earlier than those of the A components. Therefore, when we define the primary component of a WB as the heavier star of the triple system, we count eight SBs among the primary components, but 10 among the secondaries. Therefore, we agree with the recent result of Tokovinin (2015) that the frequency of SBs is the same for any component of the WBs.

Tokovinin (2008) also pointed out that, in a triple system, the close binary is usually the heaviest component of the WB. This applies also to our sample. However, this may be due to a selection effect: as noticed by Lucy & Ricco (1979), a binary star is much fainter than a single star with the same total mass, and our sample is delimited by apparent magnitude. Therefore, we cannot draw any conclusion about that question.

6.4 Correlation between the SB periods and the WB periods

The periods of the WBs are derived from our calculations in Section 5.3. They are included in Table 7. For homogeneity, we consider a possible relation between the periods of the SBs and that of the WBs for the MS stars at least as late as F5 that are not in open

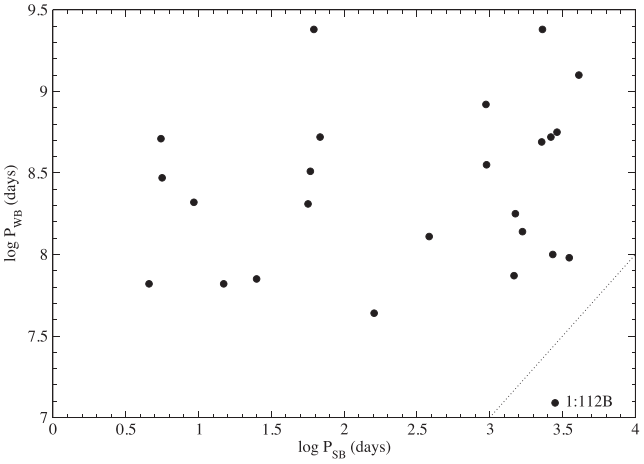

Figure 5. Period–period diagram of the 25 components of MS field WBs as late as F5, which are SBs. The dotted line is the limit $\log P_{\rm WB} > \log P_{\rm SB} + 4$.

clusters. Discarding the SBs of Table 7 with $f = 1$ or 2, one obtains the $\log P_{\rm SB}$ versus $\log P_{\rm WB}$ diagram in Fig. 5. No obvious correlation appears on this diagram. The SBs with the longest periods are components of WBs with relatively short as well as with very long periods.

In fact, this result is not in contradiction with Tokovinin (2008), who found that $\log P_{\rm WB}$ is usually less than $\log P_{\rm SB} + 4$. In Fig. 5, only one WB has a period shorter than this limit: 1:112B, in the low right corner of the figure, should have $\log P_{\rm WB}$ larger than 7.4 instead of equal to 7.09. The limitation of the SBs to periods shorter than 10 yr makes our sample unsuitable for checking Tokovinin's hypothesis.

6.5 Distribution of periods

Finally, we want to compare the distribution of periods of SBs belonging to WBs to that of close binaries as a whole. For that purpose, we consider the log-normal distribution found by Raghavan et al. (2010), which we have already used in Section 5.3. We select the SBs with a MS primary component at least as late as F5, whatever the type of the wide companion is, except those belonging to an open cluster. These SBs are indicated with an asterisk in Table 7. A comparison to the log-normal distribution until $P < 10$ yr is made with the two-sided version of Kolmogorov's test. The major distance between the cumulative distributions of periods is 0.168. For a sample of 24 objects, the probability of getting a maximum distance even larger is 48 per cent when both distributions are equal in reality. Therefore, the log-normal distribution is accepted for the SBs belonging to WBs.

7 CONCLUSION

We have carried out an observation programme, essentially with CORAVEL, to select a sample of WBs. We obtained a total of 3748 RV measurements. These observations were used to derive the orbital elements of 52 SBs (in Paper I), and to select 80 WBs with compatible RVs, parallaxes and proper motion. Adding some close WBs from list 1 of H86, we finally obtained a sample of 116 MS WBs with spectral types between F5 and M0. Moreover, 39 optical pairs were found in list 2 of H86.

The sample of MS WBs was used to derive the distribution of the separations. The constant distribution or Öpik's law was rejected, but the log-normal distribution corresponding to the period distribution of Raghavan et al. (2010) was accepted. The power law of Tokovinin & Lépine (2012), $f(a) \propto a^{-1.5}$, was widely accepted for $\log s > 3.25$. Weinberg (1990) derived from theoretical calculations that the distribution of a does not necessarily end with a break. No evidence for a break is visible in Tokovinin & Lépine (2012) until $s = 64\,000$ au, nor in our data. However, this is due to the selection of the sample: the end of the distribution could be found only by extending the search for WBs beyond the limit of T, which was applied to have a proportion of genuine WBs as large as 60 per cent. This will be possible when the *Gaia* satellite (Gaia Collaboration 2016) starts providing very accurate parallaxes, proper motions and radial velocities, and when the apparent separation will no longer be a basic criterion in the selection of WBs.

The SBs found in Paper I were used to investigate the statistical properties of the multiple systems. No correlation was found between the SBs and the WBs. The proportion of quadruple systems was compatible with a random distribution of SBs, and the SB components were equally found around the heaviest as around the lightest WB components. The first of these two results is in contrast to those of Tokovinin (2014) and Riddle et al. (2015), but their statistics include a majority of inner binaries with periods longer than 10 yr. Therefore, it seems that the environment of WBs may facilitate the formation of binaries with periods longer than a certain limit. Close binaries with periods shorter than 10 yr are not affected by this effect.

No correlation was found between the periods of the SBs and those of the WBs, but this is due to the limitation of our sample to SBs with periods until 10 yr, which is much less than the periods of the WBs.

Finally, the distribution of periods of the SBs is also compatible with that of Raghavan et al. (2010) until $P = 10$ yr.

ACKNOWLEDGEMENTS

It is a pleasure to thank Dr Thomas Maschberger for relevant information about the IMF and the mass ratio distribution. We had a fruitful email exchange with Prof Leon Lucy about the selection effects affecting the binary stars. We have benefited during the entire period of these observations from the support of the Swiss National Foundation and Geneva University. We are particularly grateful to our technicians Bernard Tartarat, Emile Ischi and Charles Maire for their dedication to the experiment for more than 20 yr. We made use of Simbad, the data base of the Centre de Données astronomiques de Strasbourg.

REFERENCES

Baranne A., Mayor M., Poncet J.-L., 1979, Vistas Astron., 23, 279
Duchêne G., Kraus A., 2013, ARA&A, 51, 269
Duquennoy A., Mayor M., 1991, A&A, 248, 485
Eggenberger A., Halbwachs J.-L., Udry S., Mayor M., 2004, Rev. Mex. Astron. Astrofis. Conf. Ser. 21, IAU Coll. 191, The Environment and Evolution of Double and Multiple Stars, ESA Publ. Div., Noordwijk, p.28
ESA 1997, The Hipparcos and Tycho Catalogues, SP-1200
Fiala A. D., 2000, in Cox A. N., ed., Allen's Astrophysical Quantities, 4th edn, AIP Press, Springer, New York, p. 12
Gaia Collaboration 2016, A&A, preprint (arXiv:1609.04153)
Halbwachs J.-L., 1986, A&AS, 66, 131 (H86)
Halbwachs J.-L., 2001, in Egret D., Halbwachs J.-L., Hameury J.-M., eds, Étoiles doubles, école thématique du CNRS, Goutelas 2000, p. 35
Halbwachs J.-L., Mayor M., Udry S., 2012, MNRAS, 422, 14 (Paper I)
Jiang Y.-F., Tremaine S., 2010, MNRAS, 401, 977

Kouwenhoven M. B. N., Goodwin S. P., Parker R. J., Davies M. B., Malmberg D., Kroupa P., 2010, MNRAS, 404, 1835
Kroupa P., Weidner C., Pflamm-Altenburg J., Thies I., Dabringhausen J., Marks M., Maschberger T., 2013, in Oswald T. D., Gilmore G., eds, Planets, Stars and Stellar Systems, vol. 5, Springer Science, Business Media, Dordrecht, p. 115
Kuiper G. P., 1935, PASP, 47, 121
Lacroute P., Valbousquet A., 1974, A&AS, 16, 343
Lépine S., Bongiorno B., 2007, AJ, 133, 889
Longhitano M., Binggeli B., 2010, A&A, 509, A46
Lucy L. B., Ricco E., 1979, AJ, 84, 401
Öpik E., 1924, Publ. de L'Obs. Astron. de l'Univ. de Tartu, XXV, n.6
Raghavan D., McAlister H. A., Henry T. J. et al., 2010, ApJS, 190, 1
Reipurth B., Mikkola S., 2012, Nature, 492, 221
Riddle R. L., Tokovinin A., Mason B. D. et al., 2015, ApJ, 799, 4
Salpeter E. E., 1955, ApJ, 121, 161
Tokovinin A. A., 2008, MNRAS, 389, 925
Tokovinin A. A., 2014, AJ, 147, 87
Tokovinin A. A., 2015, AJ, 150, 177
Tokovinin A. A., Lépine S., 2012, AJ, 144, 102
van Leeuwen F., 2007, A&A, 474, 653
Wasserman I., Weinberg M. D., 1991, AJ, 382, 149
Weinberg M. D., 1990, in Linden-Bell D., Gilmore G., eds, Mathematical and Physical Sciences, Proc. NATO Advanced Study Institute on Baryonic Dark Matter, Cambridge, UK, July 17–28 1989, Kluwer, Dordrecht, p. 117
Weinberg M. D., Shapiro S. L., Wasserman I., 1987, AJ, 312, 367
Wenger M. et al., 2000, A&AS, 143, 9

SUPPORTING INFORMATION

Additional Supporting Information may be found in the online version of this article:

Table 1. Sample of the RV catalogue. (http://www.mnras.oxfordjournals.org/lookup/suppl/doi:10.1093/mnras/stw2683/-/DC1).

Please note: Oxford University Press is not responsible for the content or functionality of any supporting materials supplied by the authors. Any queries (other than missing material) should be directed to the corresponding author for the article.

APPENDIX A: DETECTION LIMIT OF CLOSE COMPANIONS IN AGK2/3

We need the minimum separation that still allows the complete detection of the components. We consider the 780 pairs with $T < 10\,000$ yr selected when preparing H86. The distribution of these pairs according to the apparent separation and the photographic magnitude of the primary component is presented in Table A1. Each count, n_i is followed with its rate, f_i, defined as the ratio:

$$f_i = \frac{n_i}{\sum_{j \le i} n_j}, \tag{A1}$$

where j is the index of the rows from the top of the table until i included. For a given separation, it is easier to detect a companion when the primary is faint than when it is bright. Therefore, the table is presented with rows in increasing order from the faintest to the brightest magnitudes. We read each row from right to left: as long as the separation is larger than the detection limit, the rate f_i is expected to be constant (the variations are due only to Poisson noise); when the detection is not complete, f_i is decreasing. We infer from Table A1 that the radius of the image of each star, in arcseconds, is a bit less than that given by the following formula:

$$\log R_{\rm arcsec} = \frac{13 - \min(m_{\rm pg}, 10)}{7}. \tag{A2}$$

We assume that the detection is complete when the separation ρ is larger than the sum of the radii of the components.

Table A1. Search of the detection limit as a function of the photographic magnitude of the primary component, $m_{\rm pg}$, and of the apparent separation, ρ.

	ρ (arcsec)											
	<5		5–10		10–20		20–40		40–80		>80	
$m_{\rm pg}$	n_i	f_i	n_i	f_i	n_i	f_i	n_i	f_i	n_i	f_i	n_i	f_i
>10	3	1.00	29	1.00	33	1.00	16	1.00	13	1.00	66	1.00
9–10	2	0.40	17	0.37	25	0.43	19	0.54	10	0.43	107	0.62
8–9	0	0	17	0.27	19	0.25	15	0.30	22	0.49	137	0.44
7–8	1	0.17	4	0.06	13	0.14	15	0.23	19	0.30	83	0.21
6–7	0	0	0	0	7	0.07	4	0.06	4	0.06	26	0.06
5–6	0	0	0	0	4	0.04	6	0.08	2	0.03	27	0.06
4–5	0	0	0	0	0	0	1	0.01	1	0.01	9	0.02

This paper has been typeset from a TEX/LATEX file prepared by the author.